Exciton binding energies in chalcopyrite semiconductors

Bernard Gil[1,2,*] and Didier Felbacq[1,2,3]

[1]*CNRS, Laboratoire Charles Coulomb UMR 5221, F-34095 Montpellier, France*

[2]*Université Montpellier 2, Laboratoire Charles Coulomb UMR 5221, F-34095 Montpellier, France*

[3]*Institut Universitaire de France, Universite Montpellier 2, Place Eugene Bataillon, 34095 Montpellier, Cedex 5, France*

Shigefusa F. Chichibu

Center for Advanced Nitride Technology (CANTech) Institute of Multidisciplinary Research for Advanced Materials (IMRAM), Tohoku University 2-1-1 Katahira, Aoba, Sendai 980-8577, Japan

(Received 11 October 2011; revised manuscript received 5 December 2011; published 8 February 2012)

The optical spectra of Cu-III-VI_2 chalcopyrite compounds display rich excitonic features in the fundamental direct bandgap energy region. The energy structure of excited excitonic states reported in the literature are reexamined using a calculation of the eigenstates of the hydrogenic problem in the context of the anisotropic band structure and the anisotropy of the dielectric constant. We find some remarkable agreements as well as inconsistencies in the literature that we attribute to the following reasons: (i) the difficulty to interpret fine structure-splitting data in noncubic semiconductors, and (ii) the more severe difficulty growing these materials with high enough quality. We finally propose some values that match very well with recent proposals and integrate the trend between Rydberg energies and bandgap values for the binary inorganic zincblende and wurtzite semiconductors.

DOI: 10.1103/PhysRevB.85.075205 PACS number(s): 78.20.−e, 78.55.Hx, 71.35.Cc

I. INTRODUCTION

Tremendous activity is currently dedicated to the investigation of the optical properties of chalcopyrite semiconductors, in line with huge potential applications in the area of solar cell devices, for instance.[1] These materials are ordered phases of the II-IV-V_2 or I-III-VI_2 kinds. The structure of chalcopyrite is closely related to that of zincblende.[2] Bulk chalcopyrite semiconductors have been intensively studied in the 1970s for their potential nonlinear optical properties, as reviewed by Shay *et al.*[3] Their band structures and physical criteria that lead to a stable ordered phase instead of a random distribution of cations have been reviewed by Zunger.[4] From the macroscopic point of view of mineralogy and using its language, chalcopyrites are uniaxial materials; their optical properties are different when observed with light polarization parallel or perpendicular to the reversed fourfold symmetry axis of the crystal. The unit cell is twice as large, reflecting an alternation of II (resp. I) and IV (resp. III) ions replacing III (resp. II) cations in adjacent cells of the III-V (resp. II-VI) zincblende lattice and leading to space group $I\bar{4}2d$ instead of $F\bar{4}3m$. The reduction of the cubic symmetry to a quadratic one leads to a splitting of the threefold p-type spinless valence band states. From this splitting derives the anisotropy of the optical response of chalcopyrite semiconductors. In the context of a semiclassical description, most of the anisotropic optical response can be interpreted as Rowe *et al.*[5] did it in the context of a quasicubic model for the description of the p-type valence band. This simple, two-parameter model early proposed by Thomas *et al.*[6] to account for the band structure of hexagonal wurtzite II-VIs, extended to a three-parameter version, was later successfully used to interpret the optical properties of strained-layer wurtzitic nitrides.[7–9] The oscillator strength of a given optical transition, in the context of this band-to-band model, is proportional to the amount of I p_x >, I p_y > and I p_z > states in the expansion of the eigenstates of the valence band.[10] It has been also shown by Elliot[11] that including direct long-range Coulomb excitonic effects leads to substantial modification of the dielectric constant (and subsequently of the oscillator strength) compared to the band-to-band model. More recently, it was finally reported that adding short-range spin exchange interactions could furnish a dramatic correction to the oscillator strength of excitonic lines in strained layer zinc-oxide epitaxies.[12]

The calculation of excitonic binding energy in the context of anisotropic semiconductors has been accurately performed for GaSe[13] and MoS_2,[14] for wurtzitic II-VIs,[15] and more recently for group III element nitrides,[16] but it was never addressed to date in the case of chalcopyrite, for which the determination of exciton binding energies remains fairly chaotic. It is the aim of this paper to propose a method which permits us to discriminate between relevant values and inappropriate ones. For the sake of the completeness, we have to reference the very elaborate calculation which includes complementary ingredients, such as valence band mixing effects proposed by Rodina *et al.*,[17] in case of wurtzitic materials, which is very interesting. However, to be applicable, it requires the knowledge of a lot of material parameters as yet untested in the chalcopyrites.

II. METHODOLOGY

The effective mass equation for excitons then reads:

$$\left[-\frac{\hbar^2}{2m_0\mu_\parallel}\frac{\partial^2}{\partial z^2}-\frac{\hbar^2}{2m_0\mu_\perp}\left(\frac{\partial^2}{\partial x^2}+\frac{\partial^2}{\partial x^2}\right)-\frac{e^2}{4\pi\varepsilon_0}\frac{1}{\sqrt{[\varepsilon_\parallel\varepsilon_\perp(x^2+y^2)+\varepsilon_\perp^2 z^2]}}\right]\psi^\beta(r)=E^\beta\psi^\beta(r). \quad (1)$$

The eigenvalues and eigenstates of Eq. (1) are E^β and $\psi^\beta(r)$, respectively. They depend on several quantum numbers which are represented by β. The fundamental constants are the electron mass at rest m_0, the *in vacuo* dielectric constant ε_0, and the elementary electron charge e. We define the dimensionless reduced masses parallel and perpendicular to the direction of the z axis as $\mu_\parallel$ and $\mu_\perp$ respectively, and we note $\varepsilon_\parallel$ and $\varepsilon_\perp$ as the corresponding values of the relative dielectric constants. The reduced effective mass (in unit of electron mass at rest) and dielectric constant tensors (unit of ε_0) are:

$$\bar{\bar{\mu}} = \begin{pmatrix} \mu_\perp & & \\ & \mu_\perp & \\ & & \mu_\parallel \end{pmatrix}, \tag{2}$$

$$\bar{\bar{\varepsilon}} = \begin{pmatrix} \varepsilon_\perp & & \\ & \varepsilon_\perp & \\ & & \varepsilon_\parallel \end{pmatrix}, \tag{3}$$

respectively. The integration of Poisson's equation in the context of the anisotropic dielectric constant gives to the potential energy term the untrivial expression:[13–18]

$$\left[-\frac{e^2}{4\pi\varepsilon_0} \frac{1}{\sqrt{[\varepsilon_\parallel \varepsilon_\perp (x^2+y^2) + \varepsilon_\perp^2 z^2]}} \right]. \tag{4}$$

Our method consists in first rearranging this equation by making the following substitutions: $x' = x$, $y' = y$, and $z' = \sqrt{\frac{\mu_\parallel}{\mu_\perp}} z$. Second, the anisotropy parameter γ is defined as: $\gamma = \frac{\varepsilon_\perp}{\varepsilon_\parallel} \frac{\mu_\perp}{\mu_\parallel}$. Further, defining the reduced Rydberg energy: $R^* = \frac{m_0 c^2 \alpha^2}{2} \frac{\mu_\perp}{\varepsilon_\perp \varepsilon_\parallel}$, where c is the *in vacuo* light velocity and α is the fine structure constant ($\alpha = \frac{e^2}{4\pi\varepsilon_0 \hbar c} \approx \frac{1}{137}$), the in-plane radius $\rho' = \sqrt{x'^2 + y'^2}$, and the cylindrical Laplacian $\Delta(\rho', z')$, we are left solving a simple second-order differential equation:

$$\left[\Delta(\rho', z') - \frac{2}{\sqrt{\rho'^2 + \gamma z'^2}} \right] \xi^\beta(\rho', z') = \alpha^\beta \xi^\beta(\rho', z'). \tag{5}$$

In this equation, where the length unit used for ρ' and z' is an effective Bohr radius $a_\perp = \frac{4\pi\varepsilon_0 \sqrt{\varepsilon_\perp \varepsilon_\parallel} \hbar^2}{m_0 \mu_\perp e^2}$, the eigenvalues read α^β in units of R^* and the eigenstates are the $\xi^\beta(\rho', z')$ quantities.

The evolution of the long-range Coulomb energies computed vs anisotropy γ by several methods is reported in Fig. 1. From the abundant literature of the field, we have selected three different approaches. The utilization of a linear expansion of the eigenstates in terms of the hydrogenic-like states, as proposed by Baldereschi *et al.*,[14] gives results plotted using diamonds. Second, we have selected results of the calculation performed by Muljarov *et al.*,[19] using hyperspherical functions and a perturbation approach. Finally, we give the results we recently obtained by direct resolution of the problem using the finite elements method.[16] Rather than reproducing complicated mathematical calculations, we prefer to utilize a method used worldwide by engineers, namely, the finite element methods. In addition, we adapted the hydrogen atom problem directly offered by the COMSOL® software. This approach gives very rapidly accurate results, as shown in Fig. 1, and it can treat on a same footing both flattened and elongated excitons by just changing the value of the anisotropy parameter γ. Our recent successful treatment of excitons in wurtzitic semiconductors where both situations can be encountered for indicates to us that the method should be extended to chalcopyrite materials without any problem. Last, COMSOL® is very convenient since it directly offers the possibility to plot the geometric representations of the graphs of the different wave functions either with 2D or 3D aspects.[16] More information can be read in Fig. 1.

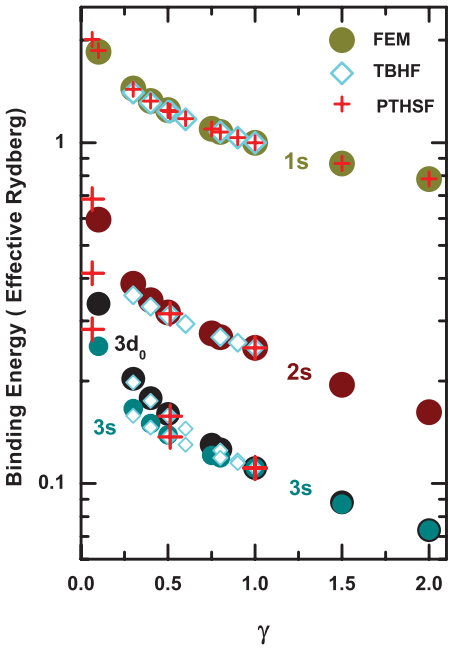

FIG. 1. (Color online) Plot of the effective Rydbergs vs anisotropy parameter γ obtained for states even under reflection in a plane through the z' axis by the finite element method (FEM, colored/gray dots), the tight-binding approach using hydrogenic functions (TBHF, open diamonds), and the perturbation theory using hyperspherical functions (PTHSF, red/dark gray crosses). According to the cylindrical symmetry, the eigenstates have to be classified in accordance with the irreducible representations of the cylindrical group D_∞^h. The degeneracy in terms of angular momentum is lifted away from $\gamma = 0$ and $\gamma = 1$, which gives the splitting between $3s$ and $3d_0$ (we have kept here the notations of spherical symmetry for the sake of the simplicity, which is not appropriate in the strictest sense).

First, we note the evolution of the $1s$ exciton binding energy, which increases when $\gamma \to 0$ and decreases when $\gamma > 1$ {note that in the case of both three-dimensional ($\gamma = 1$) and two-dimensional ($\gamma = 0$) situations the energy spectra of hydrogenic series are degenerated vs angular momentum values. They can be expressed as a function of the principal quantum number n as $\frac{R}{n^2}$ and $\frac{R}{[n-\frac{1}{2}]^2}$, respectively[20]}.

Second, we note that the degeneracy of the $n = 3$ state with the value of the angular momentum is suppressed; different energies are computed for $3s$ and $3d_0$ states when $\gamma \neq 1$, as expected by group theory.[14–16] We have restricted the plot in Fig. 1 to eigenstates that are even under reflexion in a plane through the z' axis, which are the states that are radiative, but we wish to emphasize the fact that the calculation leads to splittings between $2s$-, $2p_0$-, and $2p_{\pm 1}$-like states (eigenstates

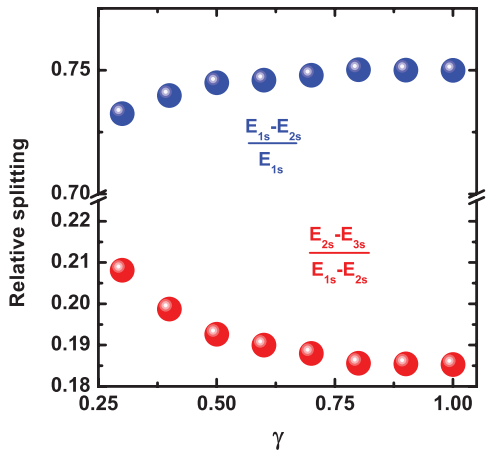

FIG. 2. (Color online) Plot of the $1s$-$2s$ splitting energy relative to the $1s$ binding energy vs anisotropy parameter γ (blue/gray dots, upper plot). Plot of the $2s$-$3s$ splitting energy relative to the value of the $1s$-$2s$ splitting energy vs anisotropy parameter γ (red/dark gray dots, lower plot).

that are odd under reflexion in a plane through the z' axis) when $\gamma \neq 1$. The oscillator strength of $3d_0$ states remains very small[14] compared with the oscillator strength of $3s$ ones. The evolution of the splitting between $1s$ and $2s$ exciton states relative to the value of the $1s$ binding energy is interesting to plot when the anisotropy changes. In the case of a spherical ($\gamma = 1$) situation, this splitting is 0.75 times the binding energy, while it becomes 0.745 when $\gamma = 0.5$ and 0.793 when $\gamma = 2$. The evolution of this splitting as well as the evolution of the $2s$-$3s$ splitting relative to the $1s$-$2s$ one has been plotted in Fig. 2. This information is crucial for the determination of the exciton binding energy in anisotropic semiconductors from the measurement of the splitting between $1s$, $2s$, and $3s$ excitonic features after a step-by-step procedure. First, the value of the $2s$-$3s$ splitting expressed relatively to the value of the $1s$-$2s$ splitting permits us to obtain the value of γ, as shown in Fig. 2. This value of γ will further lead to the values of the excitonic binding energy E_{1s} from the evolution of $\frac{E_{1s}-E_{2s}}{E_{1s}}$ vs γ. Of course, the procedure only holds when three excitonic transitions are measured, which is the Achille's heel of the method. Measuring the excitonic splittings in semiconductor materials is not so easy. It requires single crystals of high structural quality with values of the radiative inhomogeneous and nonradiative homogeneous broadenings of the excitonic lines that are smaller than the excitonic splittings.

III. DATA ANALYSIS

A. $CuInS_2$

To illustrate these considerations from a more quantitative point of view, let us consider, for instance, $CuInS_2$, for which there are measured excitonic features at 1.5355, 1.5494, and 1.5532 eV for the $1s$, $2s$, and $3s$ excitons, respectively.[21] The ratio between the value of the $2s$-$3s$ splitting relative to the $1s$-$2s$ splitting equals 0.274, which according to our calculation gives an anisotropy parameter of about 0.1, a value much smaller than what was reported for wurtzitic nitrides[16] (between 0.74 and 1.8), wurtzitic II-VI compounds (values between 0.75 and 1.16),[15] III-VI compounds like GaSe (0.6),[14] and layer compounds like MoS_2 (0.2 and 0.3).[14] For such an anisotropy, the $1s$-$2s$ splitting is about 68% of the $1s$ binding energy (see Fig. 2). From the 13.9-meV value of the $1s$-$2s$ splitting measured for $CuInS_2$, we calculate an exciton binding energy of 20.48 meV, a value significantly higher than the proposed value (18.5 meV), which was obtained in the context of a spherical description of the excitonic series. This 20.5-meV value is in agreement with the quenching of photoluminescence with temperature.[22] Another group[23] had earlier reported energies at 1.5322, 1.5743, and 1.5821 eV measured by wavelength-modulated reflectivity. The ratio we obtain for the value of the $2s$-$3s$ splitting relative to the $1s$-$2s$ splitting equals 0.185, leading to an anisotropy parameter of 0.05. Relative to the $1s$ binding energy, the $1s$-$2s$ splitting equals about 63% of the exciton binding energy, which gives and exciton binding energy at 67 meV. The disagreement between the two groups resides in the interpretation of the 1.5494 line attributed to the $n = 2$ state of the A exciton by the first group, which is measured at 1.5496 eV, and the $1s$ state of the B exciton by the second group. Polarization experiments[21] plead in favor of a weak exciton binding energy,[22] and we have to disregard the proposal of a strong excitonic binding energy[23] in reason of an unfortunate misinterpretation of extremely rich experimental spectra.

B. $CuGaS_2$

Excitonic transitions associated with $n = 1$, 2, and 3 excitons were measured at 2.4995, 2.525, and 2.530 eV in $CuGaS_2$.[23] The ratio we obtain for the value of the $2s$-$3s$ splitting relative to the $1s$-$2s$ splitting equals 0.196, leading to an anisotropy parameter of 0.45 and a $1s$-$2s$ energy splitting of 74.2% of the exciton binding energy. Using the hydrogenic model, the authors suggest a 33-meV exciton binding energy. We obtain 34.4 meV in this sample, which is a 4% enhancement. Shirakata *et al.*[24] had earlier reported an excited state photoluminescence peak at 2.525 eV (see Fig. 4 of Ref. 24). Excitonic transitions have also been measured in $CuGaS_2$ at energies of 2.5011, 2.5303, and 2.5357 eV for the $1s$, $2s$, and $3s$ excitons, respectively (see Table I in Ref. 25). The $1s$-$2s$ splitting equals 29.2 meV, and the $2s$-$3s$ splitting equals 5.4 meV. The ratio we compute equals 0.185, leading to an anisotropy parameter of 1.05. The exciton binding energy can be obtained using the hydrogenic model, which leads to 38 meV.

C. $CuGaSe_2$

Four fluorescence maxima have been reported in the fluorescence spectrum of $CuGaSe_2$[26] at 1.7241, 1.7500,1.7550, and 1.7568 eV, which were attributed to the $n = 1$, 2, 3, and 4 states of the exciton, respectively, leading to a 5-meV value for the $3d_0$-$2s$ splitting and a 6.8-meV value for the $3s$-$2s$ splitting. The ratio 6/25.9 equals 0.262, which corresponds to an anisotropy parameter of about 0.12 and a $1s$-$2s$ splitting of 67% of the exciton binding energy. The exciton binding energy is then estimated at about 39 meV for the A exciton, which constitutes a 1-meV increase with respect to the initial proposal.

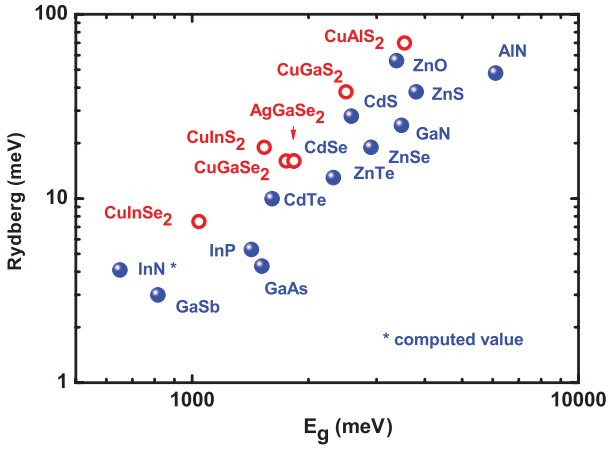

FIG. 3. (Color online) Plot of the excitonic binding energy vs fundamental direct bandgap for most common III-V and II-VI semiconductors (blue/gray dots) and for the chalcopyrite semiconductors we study here (open red/dark gray dots).

We remark that Bauknecht *et al.*[27] and Luckert *et al.*[28] alternatively proposed values in the 14-meV range, in agreement with the initial proposal by Chichibu *et al.*[29] This large scattering of data is the evidence of severe material problem issues or misinterpretation of experimental data which we have not understood, but a proposal will be made later.

D. $CuInSe_2$

Nemerenco[30] has reported detailed investigation of the excitonic reflectivity of $CuInSe_2$ crystals. The energies of the three lowest excitonic transitions attributed to the Γ_7 valence band (A excitons) are 1.0369, 1.0662, and 1.0716 eV. The value of the $1s$-$2s$ splitting is 29.3 meV, and the value of the $2s$-$3s$ splitting is 5.4 meV. The ratio we compute equals 0.185, leading to an anisotropy parameter of 1.05. The corresponding value of the exciton binding energy is 39.1 meV. The energies of the three excitonic transitions attributed to the Γ_6 valence band (B excitons) are 1.0431, 1.0703, and 1.0754 eV. The value of the $1s$-$2s$ splitting is 27.2 meV, and the value of the $2s$-$3s$ splitting is 5.1 meV. The ratio we compute equals 0.19, leading to an anisotropy parameter of 0.6, which gives an exciton binding energy at 1.34 times the $1s$-$2s$ splitting; that is to say at 36.5 meV. These interpretation are challenged by several recent experimental investigations, such as photoluminescence quenching with temperature,[31,32] magnetophotoluminescence,[33] which all plead in favor an exciton binding energy sitting at about 8 meV. Our opinion is that interpretation of data in Fig. 1 of Ref. 30. has to be rehandled in particular since transition at 1.05 eV has not been attributed and is most probably due to erroneous valence band ordering. According to selection rules, Chichibu *et al.*[31] had proposed a valence band ordering of the sequence Γ_6-Γ_7-Γ_7, which is the analogous *mutatis mutandis* to the unstrained GaN case[8] for $CuInSe_2$, at variance with the proposal of Ref. 30.

At this stage, we try to propose values which are from bona fide compatible to the trends reported for many semiconductors. The 36–39-meV values of the binding energies proposed for $CuInSe_2$ are particularly large compared with the trend in semiconductors reported in Fig. 3, where we have plotted the excitonic binding energies vs bandgap. The exciton binding energies in binary semiconductor compounds are plotted in blue, while the values for Cu-(Ga,In) VI_2 chalcopyrite ones are plotted in red. We have also included for completeness the $CuAlS_2$ value that is believed to sit near 70 meV[34] and the AgGaSe2 one proposed at 16 meV.[35] The figure phenomenologically indicates that the exciton binding energy cannot sit at 39 meV for $CuInSe_2$ but is located in the 7.5–8-meV range instead. Similar arguments plead in favor of a 15-meV value for the excitonic binding energy in $CuGaSe_2$. The figure also indicates that, given a bandgap energy, the largest binding energy in the series of fourfold coordinated semiconductors are observed in the case of chalcopyrite semiconductors because the valence bands of chalcopyrite semiconductors studied here are raised due to the repulsion from the Cu-3d band. Thus the universal line in Fig. 3 is down-shifted horizontally.

IV. CONCLUSIONS

In conclusion, we have interpreted the splittings attributed to different excitonic levels previously measured in a large variety of chalcopyrite semiconductors which have furnished sufficient information to do so. We find either a good agreement or a very bad one. However, careful analysis of the literature permits us to keep the correct values for some materials in some cases and to reject the proposed ones for others. Such a discrepancy is attributed to sometimes moderate material quality, to the difficulty of identifying a given transition in the context of the complexity of the valence band structure (there are both crystal and field spin-orbit splittings in these quadratic materials) when excited states associated with a given valence band may overlap with ground states of another one. However, selection rules that govern the optical transitions could sometimes permit discrimination between relevant and questionable proposals. We anticipate that modern epitaxial methods should rapidly furnish high layers with different strain fields and orientations in order to allow measuring optical properties with clear selection rules, as it has been the case for nitrides. It is worthwhile noticing, however, that with the improvements of the crystalline qualities, materials parameters will be better known. At that time, it will be obviously necessary to escape from the calculation of the excitonic binding energies in the context of the one-band approximation. More elaborate approaches, including the full valence structure, crystal field splitting, and spin-orbit interactions, like the one proposed for wurtzitic semiconductors by Rodina *et al.*,[17] will be applicable in order to reach a final understanding of exciton binding energies in chalcopyrite semiconductors. Then the question of the exciton binding energies, including their dependencies with strain, will be rapidly and unambiguously solved in chalcopyrites.

ACKNOWLEDGMENTS

This work was done within the financial support of CNRS under Contract PEPS ANISEXCIT.

*Corresponding author: Laboratoire Charles Coulomb, Universite Montpellier 2, Place Eugene Batallion, 34095 Montpellier, Cedex 5, France; bernard.gil@univ-montp2.fr

[1]For a recent review, see for instance, *Wide Bandgap Chalcopyrite*, edited by S. Siebentritt and U. Rau (Springer Verlag, Berlin, Heidelberg, 2006), p. 14.

[2]C. L. Burdick and James H. Ellis, Proc. Natl. Acad. Sci. USA **3**, 644 (1917).

[3]J. L. Shay and J. H. Wernick, *Ternary Chalcopyrite Semiconductors* (Pergamon, New York, 1975), p. 25.

[4]A. Zunger, Mater. Res. Bull. **22**, 20 (1997) and references therein.

[5]J. E. Rowe and J. L. Shay, Phys. Rev. **3**, 451 (1972).

[6]D. G. Thomas and J. J. Hopfield, Phys. Rev. **128**, 2135 (1962).

[7]R. Dingle, D. D. Sell, S. E. Stokowski, and M. Ilegems, Phys. Rev. B **4**, 1211 (1971).

[8]B. Gil, O. Briot, and R. L. Aulombard, Phys. Rev. B **52**, 17028 (1995).

[9]S. Chichibu, A. Shikanai, T. Azuhata, T. Sota, A. Kuramata, K. Horino, and S. Nakamura, Appl. Phys. Lett. **68**, 3766 (1996).

[10]B. Gil, F. Hamdani, and H. Morkoç, Phys. Rev. B **54**, 7678 (1996).

[11]R. J. Elliot, Phys. Rev. **108**, 1384 (1957).

[12]B. Gil, Phys. Rev. B **64**, 201 (2001); B. Gil, A. Lusson, V. Sallet, Said-Assoumani Said-Hassani, R. Triboulet, and P. Bigenwald, Jpn. J. Appl. Phys. Lett. **40**, L1089 (2001).

[13]R. G. Wheeler and J. O. Dimmock, Phys. Rev. **125**, 1805 (1965).

[14]A. Baldereschi and M. G. Diaz, Il Nuovo Cimento B **68**, 217 (1970).

[15]N. O. Lipari, Phys. Rev. B **4**, 4535 (1971).

[16]B. Gil and D. Felbacq, Phys. Status Solidi B (to be published).

[17]A. V. Rodina, M. Dietrich, A. Göldner, L. Eckey, A. Hoffmann, Al. L. Efros, M. Rosen, and B. K. Meyer, Phys. Rev. B **64**, 115204 (2001).

[18]For a general demonstration, see for instance, L. D. Landau and E. M. Lifshitz, *Electrodynamics of Continuous Media*, the Course of the Theoretical Physics Vol. VIII, 2nd rev. ed. (Pergamon Press, Moscow, 1984), p. 56.

[19]E. A. Muljarov, A. L. Yablonskii, S. G. Tikhodeev, A. E. Bulatov and J. L. Birman, J. Math. Phys. **41**, 6026 (2000).

[20]S. Flügge and H. Marshall, *Rechenmethoden der Quantentheorie* (Springer, Berlin, 1965), p. 80.

[21]A. V. Mudryi, A. V. Ivanyukovich, M. V. Yakushev, R. Martin, and A. Saad, Semiconductors **42**, 29 (2008).

[22]M. V. Yakushev, R. W. Martin, A. V. Mudryi, and A. V. Ivanyukovich, Appl. Phys. Lett. **92**, 111908 (2008).

[23]N. N. Syrbu, I. M. Tiginyanu, L. L. Nemerenco, V. V. Ursaki, V. E. Tezlevan, and V. V. Zalamai, J. Phys. Chem. Solids **66**, 1974 (2005).

[24]S. Shirakata, K. Saiki, and S. Isomura, J. Appl. Phys. **68**, 291 (1990).

[25]N. N. Syrbu B. V. Korzun, A. A. Fazeyeva, R. R. Mianzelen, V. V. Ursaki, and I. Galbic, Phys. B **405**, 3243 (2010), and reference therein.

[26]S. Levchenko, N. N. Syrbu, V. E. Tezlevan, E. Arushanov, J. M. Merino, and M. Leon, J. Phys. D **41**, 055403 (2008).

[27]A. Bauknecht, S. Siebentritt, J. Albert, Y. Tomm, and M. C. Lux-Steiner, Jpn. J. Appl. Phys. **39**, 322 (2000).

[28]F. Luckert, M. V. Yakushev, C. Faugeras, A. V. Karotki, A. V. Mudryi, and R. W. Martin, Appl. Phys. Lett. **97**, 162101 (2010).

[29]S. Chichibu, T. Mizutani, K. Murakami, T. Shioda, T. Kurafuji, H. Nakanishi, S. Niki, P. J. Pons, and A. Yamada, J. Appl. Phys. **83**, 3678 (1998).

[30]L. Nemerenco, Moldavian J. Phys. Sci. **4**, 4 (2005).

[31]M. V. Yakushev, F. Luckert, C. Faugeras, A. V. Karotki, A. V. Mudryi, and R. W. Martin, Jpn. J. Appl. Phys. **50**, 05FC03 (2011).

[32]M. V. Yakushev, R. W. Martin, and A. V. Mudryi, Phys. Status Solidi C **6**, 1082 (2009).

[33]M. V. Yakushev, R. W. Martin, A. Babinski, and A. V. Mudryi, Phys. Status Solidi C **6**, 1086 (2009).

[34]*Introduction to Nitride Semiconductor Blue Lasers and Light emitting Diodes*, edited by S. Nakamura and S. F. Chichibu (Taylor and Francis, London and New York, 2000) Ch. 5, p. 164.

[35]I. V. Bodnar and M. V. Yakushev, Tech. Phys. **49**, 335 (2004), translated from Zhurnal Teknicheskoi Fiziki **74**, 55 (2004).